First publ. in: Chemistry and Physics of Lipids 141 (2006), 1-2, pp. 30-47

Folding kinetics of the outer membrane proteins OmpA and FomA into phospholipid bilayers

Jörg H. Kleinschmidt *

Fachbereich Biologie, Fach M 694, Universität Konstanz, D-78457 Konstanz, Germany

Abstract

The folding mechanism of outer membrane proteins (OMPs) of Gram-negative bacteria into lipid bilayers has been studied using OmpA of *E. coli* and FomA of *F. nucleatum* as examples. Both, OmpA and FomA are soluble in unfolded form in urea and insert and fold into phospholipid bilayers upon strong dilution of the denaturant urea. OmpA is a structural protein and forms a small ion channel, composed of an 8-stranded transmembrane β-barrel domain. FomA is a voltage-dependent porin, predicted to form a 14 stranded β-barrel. Both OMPs fold into a range of model membranes of very different phospholipid compositions. Three membrane-bound folding intermediates of OmpA were discovered in folding studies with dioleoylphosphatidylcholine bilayers that demonstrated a highly synchronized mechanism of secondary and tertiary structure formation of β-barrel membrane proteins. A study on FomA folding into lipid bilayers indicated the presence of parallel folding pathways for OMPs with larger transmembrane β-barrels.

Keywords: Membrane protein folding; Outer membrane proteins; OmpA; FomA; Membrane protein chaperones; Lipid–protein interactions; Lipopolysaccharide; Protein insertion

Contents

Abbreviations: CD, circular dichroism; CCA, critical concentration for assembly; CMC, critical micelle concentration; *di*$C_{10:0}$PC, 1,2-dicapryl-*sn*-glycero-3-phosphocholine; *di*$C_{11:0}$PC, 1,2-diundecanoyl-*sn*-glycero-3-phosphocholine; *di*$C_{12:0}$PC, 1,2-lauryl-*sn*-glycero-3-phosphocholine; *di*$C_{14:0}$PC, 1,2-dimyristoyl-*sn*-glycero-3-phosphocholine; *di*$C_{18:1}$PC, 1,2-dioleoyl-*sn*-glycero-3-phosphocholine; FomA, major outer membrane protein A; IMP, integral membrane protein; KTSE, kinetics of tertiary and quarternary structure formation determined by electrophoresis; LDAO, *N*-lauroyl-*N*,*N*-dimethylammonium-*N*-oxide; LUVs, large unilamellar vesicles; OMP, outer membrane protein; OmpA, outer membrane protein A; SDS, sodium dodecyl sulfate; PAGE, polyacrylamide gel electrophoresis; SUVs, small unilamellar vesicles

* Tel.: +49 7531 88 3360; fax: +49 7531 88 3183.
E-mail address: joerg.helmut.kleinschmidt@uni-konstanz.de.

1. Introduction

In recent years, investigations on folding and membrane insertion of outer membrane proteins (OMPs) into lipid bilayers were performed using the outer membrane protein A (OmpA) of *Escherichia coli* (Kleinschmidt et al., 1999a, 1999b; Kleinschmidt and Tamm, 1996, 1999, 2002; Surrey and Jähnig, 1992, 1995) and the major outer membrane porin (FomA) of *Fusobacterium nucleatum* (Pocanschi et al., 2006) as examples. All currently known OMPs of bacteria have β-sheet secondary structure in the transmembrane region and no transmembrane helices facing the lipid bilayer. The transmembrane strands of OMPs are connected by short periplasmic β-turns and by long loops facing the polysaccharide region and the space outside the cell. The geometry of the β-strands and the necessity to form hydrogen bonds between polar amide and carbonyl groups of the polypeptide chain within the hydrophobic core of the membrane excludes that individual β-strands can exist in a lipid bilayer. Therefore all known integral membrane proteins with transmembrane β-strands form barrel structures, in which neighboring β-strands are connected by hydrogen bonds. The β-barrel is characterized by the number of antiparallel β-strands and by the shear number, which is a measure for the inclination angle of the β-strands against the barrel axis. The OMPs of bacteria of known crystal structure form transmembrane β-barrels with even numbers of β-strands ranging from 8 to 22 with shear numbers from 8 to 24 (Schulz, 2002). The strands are tilted by 36° to 44° relative to the barrel axis (Marsh and Páli, 2001; Schulz, 2002). Some OMPs of known crystal structure are listed in Table 1 and some structures are shown in Fig. 1. Outer membrane proteins exist as monomers (for example OmpA, FhuA), dimers (OmPlA) or trimers (OmpF, LamB). In the transmembrane β-strands, only every second amino acid faces the apolar lipid phase and must be a hydrophobic residue, while the others face the interior of the β-barrel and are mostly polar. Therefore, the average hydrophobicity of transmembrane β-barrels is low. According to their functions, OMPs can be grouped into at least 10 different categories. OMPs may serve as structural proteins (for example OmpA), as toxin binding proteins (OmpX), as passive unspecific diffusion porines (OmpF, OmpC), as specific porines (LamB, ScrY, FadL, Tsx), as active transporters (FhuA, BtuB), as proteases (OmpT), lipases (OmPlA), or acyltransferases (PagP), as adhesion proteins (NspA, OpcA), or as export channels (TolC). Some OMPs of known crystal structure are listed in Table 1, together with their molecular weights, p*I*, number of transmembrane β-strands, number of amino acid residues, oligomeric state and function.

2. Detergent micelles and lipid bilayers induce folding of β-barrel membrane proteins

Henning and coworkers demonstrated that the denatured integral membrane protein OmpA develops native structure when incubated with lipopolysaccharide (LPS) and Triton X-100 detergent after dilution of the denaturants sodium dodecyl sulfate (SDS) or urea (Schweizer et al., 1978). Similarly, Dornmair et al. (1990) showed that OmpA that was unfolded by heating it in SDS micelles, regained native structure when incubated in micelles of the detergent octylglucoside even in absence of LPS. These results on the β-barrel OmpA and the successful refolding of bacteriorhodopsin that consists of a bundle of seven transmembrane α-helices and was first refolded by Khorana and coworkers in 1981 (Huang et al., 1981), suggest that the information for the formation of native structure in integral membrane proteins is contained in their amino acid sequence, as previously described by the Anfinsen paradigm for soluble proteins (Anfinsen, 1973), but requires the hydrophobic environment of micelles or bilayers.

To determine basic principles for the folding of β-barrel membrane proteins, folding of OmpA was investigated with 64 detergents and phospholipids that had very different compositions of the polar headgroup, did not carry a net charge, and had a hydrophobic carbon chain length ranging from 7 to 14 carbons (Kleinschmidt et al.,

Table 1
Examples of outer membrane proteins of known high-resolution structure

OMP	Organism	MW (kDa)	p*I*	Residues	Residues in β-barrel domain	β-strands in barrel domain	Oligomeric state	Function	PDB entry	Reference
Outer membrane proteins with single-chain β-barrels										
OmpA	*E. coli*	35.2	5.6	325	171	8	Monomer	Structural	1QJP, 1BXW	Pautsch and Schulz (1998) and Pautsch and Schulz (2000)
OmpA[a]	*E. coli*	35.2	5.6	325	171	8	Monomer	Structural	1G90	Arora et al. (2001)
OmpX	*E. coli*	16.4	5.3	148	148	8	Monomer	Toxin binding	1QJ8	Vogt and Schulz (1999)
OmpX[a]	*E. coli*	16.4	5.3	148	148	8	Monomer	Toxin binding	1Q9F	Fernandez et al. (2004)
NspA	*Neisseria meningitidis*	16.6	9.5	153	153	8	Monomer	Cell adhesion	1P4T	Vandeputte-Rutten et al. (2003)
PagP	*E. coli*	19.5	5.9	166	166	8	Monomer	Palmitoyl transferase	1HQT	Ahn et al. (2004)
PagP[a]	*E. coli*	19.5	5.9	166	166	8	Monomer	Palmitoyl transferase	1MM4, 1MM5	Hwang et al. (2002)
OmpT	*E. coli*	33.5	5.4	297	297	10	Monomer	Protease	1I78	Vandeputte-Rutten et al. (2001)
OpcA	*N. meningitidis*	28.1	9.5	254	254	10	Monomer	Adhesion protein	1K24	Prince et al. (2002)
Tsx	*E. coli*	31.4	4.9	272	272	12	Monomer	Nucleoside uptake	1TLW, 1TLY	Ye and van den Berg (2004)
NalP	*N. meningitidis*	111.5	6.7	1063	267	12	Monomer	Autotransporter	1UYN	Oomen et al. (2004)
OmPlA	*E. coli*	30.8	5.1	269	269	12	Dimer	Phospholipase	1QD6	Snijder et al. (1999)
FadL	*E. coli*	45.9	4.9	421	378	14	Monomer	Fatty acid transporter	1T16, 1T1L	van den Berg et al. (2004)
Omp32	*Comamonas acidovorans*	34.8	8.8	332	332	16	Trimer	Porin	1E54	Zeth et al. (2000)
Porin	*Rhodobacter capsulatus*	31.5	4.0	301	301	16	Trimer	Porin	2POR	Weiss et al. (1991) and Weiss and Schulz (1992)
Porin	*Rhodopseudomonas Blastica*	30.6	3.8	290	290	16	Trimer	Porin	1PRN	Kreusch and Schulz (1994)
OmpF	*E. coli*	37.1	4.6	340	340	16	Trimer	Porin	2OMF	Cowan et al. (1992)
PhoE	*E. coli*	36.8	4.8	330	330	16	Trimer	Porin	1PHO	Cowan et al. (1992)
OmpK36	*Klebsiella pneumoniae*	37.6	4.4	342	342	16	Trimer	Porin	1OSM	Dutzler et al. (1999)
LamB	*E. coli*	47.4	4.7	420	420	18	Trimer	Maltose specific porin	1MAL, 1AF6	Schirmer et al. (1995) and Wang et al. (1997)
Maltoporin	*Salmonella typhimurium*	48.0	4.7	427	427	18	Trimer	Maltose specific porin	2MPR	Meyer et al. (1997)
ScrY	*S. typhimurium*	53.2	5.0	483	415	18	Trimer	Sucrose porin	1A0S, 1A0T	Forst et al. (1998)
FhuA	*E. coli*	78.7	5.1	714	587	22	Monomer	Ferrichrome iron transporter	2FCP, 1BY3	Ferguson et al. (1998) and Locher et al. (1998)
FepA	*E. coli*	79.8	5.2	724	574	22	Monomer	Ferrienterobactin transporter	1FEP	Buchanan et al. (1999)
FecA	*E. coli*	81.7	5.4	741	521	22	Monomer	Iron (III) dicitrate transporter	1KMO, 1PNZ	Ferguson et al. (2002) and Yue et al. (2003)
BtuB	*E. coli*	66.3	5.1	594	459	22	Monomer	Vitamin B_{12} transporter	1NQE, 1UJW	Chimento et al. (2003) and Kurisu et al. (2003)
FpvA	*Pseudomonas aeruginosa*	86.5	5.1	772	538	22	Monomer	Ferripyoverdine transporter	1XKH	Cobessi et al. (2005)

OMP	Organism	MW (kDa)	p*I*	Residues	Residues in β-barrel domain	β-strands in barrel domain	Chains in the β-barrel	Function	PDB entry	Reference
Outer membrane proteins with multi-chain β-barrels										
TolC	*E. coli*	51.5	5.2	471	285 (95 × 3)	12 (4 × 3)	Trimer	Export channel	1EK9	Koronakis et al. (2000)
MspA	*M. smegmatis*	17.6	4.4	168	432 (32 × 8)	16 (2 × 8)	Octamer	Porin	1UUN	Faller et al. (2004)
α-Hemolysin	*S. aureus*	33.2	7.9	293	378 (54 × 7)	14 (2 × 7)	Heptamer	Toxin	7AHL	Song et al. (1996)

[a] NMR structure.

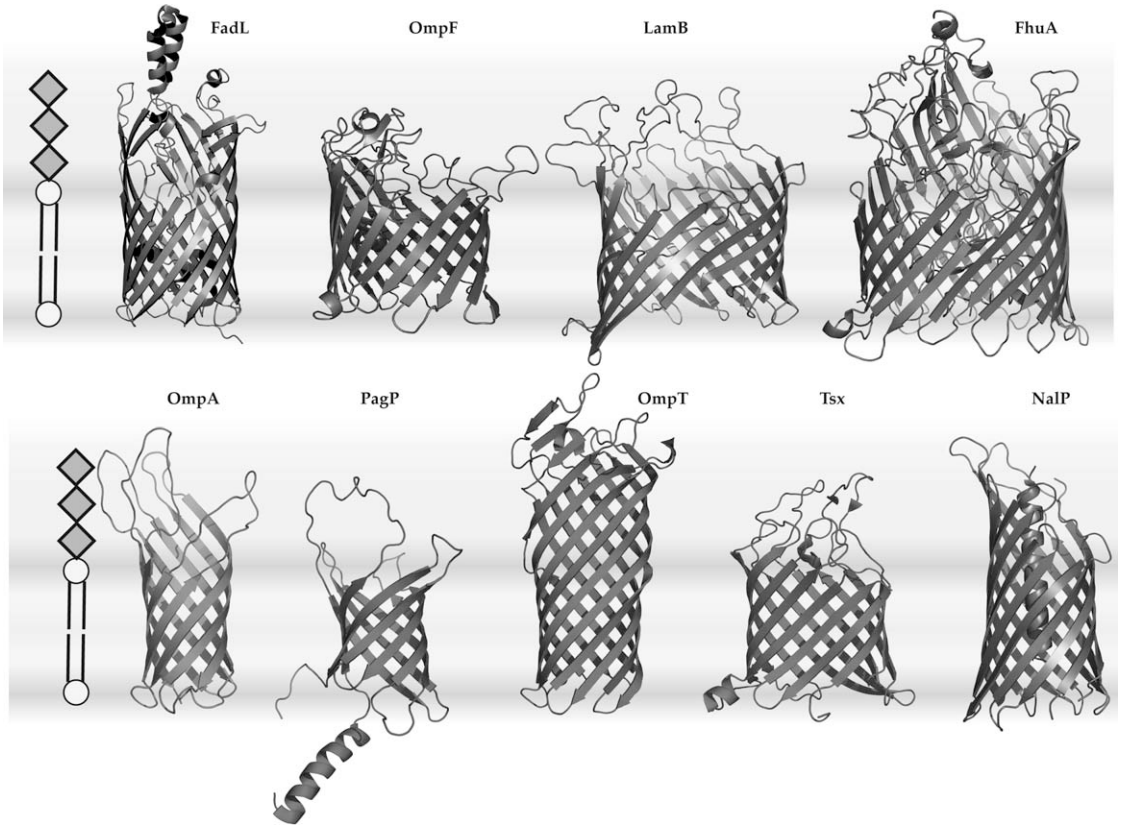

Fig. 1. PDB structures of some β-barrel membrane proteins of the outer membranes of bacteria are shown. The β-barrel domains of these OMPs have an even number of antiparallel TM strands, which is 8 for OmpA (Pautsch and Schulz, 1998, 2000; Arora et al., 2001), 8 for PagP (Ahn et al., 2004; Hwang et al., 2002), 10 for OmpT (*1I78* (Vandeputte-Rutten et al., 2001)), 12 for Tsx (*1TLW* (Ye and van den Berg, 2004)) and NalP (*1UYN* (Oomen et al., 2004)), 14 for FadL (*1T16* (van den Berg et al., 2004)), 16 for OmpF (*2OMF* (Cowan et al., 1992)), 18 for LamB (*1MAL* (Schirmer et al., 1995)), and 22 for FhuA (*2FCP* (Ferguson et al., 1998)). OmpA is a structural protein and a small ion channel (Arora et al., 2000), PagP is a palmitoyl transferase, OmpT is a protease, Tsx is a nucleoside channel, NalP is an autotransporter, FadL is a long chain fatty acid transporter, OmpF is a diffusion pore, LamB is a maltose specific porin, and FhuA an active transporter for ferrichrom iron. OMPs of mitochondria are predicted to form similar TM β-barrels. Examples are the VDAC channels, out of which more than a dozen have been sequenced (Heins et al., 1994). Protein structures were generated with Pymol (Delano, 2002).

1999b). The experiments demonstrated that for OmpA folding, it was only necessary that the concentrations of these detergents or phospholipids were above the critical micelle concentration (CMC), demonstrating that a supramolecular assembly, i.e. micelles or lipid bilayers, with a hydrophobic interior is the minimal requirement for the formation of a β-barrel transmembrane domain. However, OmpA did not fold into micelles of sodium dodecyl sulfate (SDS), which have a strong negative surface charge. When OmpA folding was monitored by circular dichroism (CD) spectroscopy and by electrophoretic mobility measurements (Kleinschmidt et al., 1999b), these methods indicated that OmpA assumes either both, secondary and tertiary structure (i.e. the native state) or no structure at all after exposure to amphiphiles with short hydrophobic chains with 14 or fewer carbons. Structure formation depended on the presence of supramolecular assemblies (micelles, bilayers). OmpA folding into micelles is a thermodynamically controlled two state process (Hong and Tamm, 2004; Kleinschmidt et al., 1999b). The necessary presence of amphiphiles (lipids, detergents) above the critical concentration for assembly (CCA[1]) to induce the formation of native secondary and tertiary structure in OmpA, also indicated that β-barrel structure does not develop while

[1] The term critical concentration for assembly (CCA) is defined here to describe the amphiphile concentration at which a geometrically unique, water-soluble supramolecular assembly is formed, which can be a micelle, a lipid vesicle, or even an inverted or cubic lipid phase. The CCA is identical with the critical micelle concentration (CMC) in the special case of micelle forming detergents. The CCA does not refer to the formation of random aggregates (for instance of misfolded membrane proteins).

detergent or lipid monomers are adsorbed to a newly formed hydrophobic surface of the protein. To the contrary, a hydrophobic core of a micelle or bilayer must be present to allow folding of OmpA. Similar observations were reported later for another outer membrane protein, OmpG (Conlan and Bayley, 2003) that folded into a range of detergents such as Genapol X-080, Triton X-100, *n*-dodecyl-β-D-maltoside, Tween 20, and octylglucoside. However, OmpG did neither fold into *n*-dodecylphosphocholine nor into the negatively charged detergents SDS and sodium cholate. Similar to OmpA, the detergent concentrations had to be above the critical micelle concentration for OmpG folding (Conlan and Bayley, 2003). A range of other OMPs has been successfully refolded into detergent micelles and subsequently crystallized, for a review see (Buchanan, 1999).

3. Oriented insertion and folding into phospholipid bilayers

In contrast to micelles, bilayers contain a much larger number of molecules and they are tightly packed. Lipid bilayers form the backbone of biological membranes and are therefore better model systems for the study of insertion and folding than detergent micelles. Surrey and Jähnig (1992) were first to report that an unfolded outer membrane protein (OmpA) spontaneously inserts and folds into phospholipid bilayers after dilution of the denaturant urea. Oriented insertion and folding of OmpA into lipid bilayers in absence of detergent was observed when unfolded OmpA in 8 M urea was reacted with small unilamellar vesicles (SUVs) of dimyristoyl phosphatidylcholine (*di*$C_{14:0}$PC) under concurrent strong decrease of the urea concentration. The OmpA insertion into bilayers of *di*$C_{14:0}$PC was oriented, because proteolysis of OmpA with trypsin led to a 24 kDa fragment, while the full-length OmpA (35 kDa) was no longer detected. A translocation of the periplasmic domain of OmpA across the lipid bilayer to the vesicle inside would have lead to a full protection of OmpA from proteolysis. The 24 kDa fragment corresponded to the membrane inserted β-barrel domain (19 kDa) and a smaller part of the periplasmic domain inaccessible to the protease. In contrast to direct insertion of OmpA into lipid bilayers, only 50% of detergent-refolded OmpA that was reconstituted into *di*$C_{14:0}$PC vesicles after refolding into micelles, could be cleaved with trypsin, indicating random orientation of the periplasmic domain inside and outside of the phospholipid vesicles (Surrey and Jähnig, 1992). It is therefore unlikely that OmpA would first fold into LPS micelles in the periplasm, which then fuse with the outer membrane as first proposed for PhoE based on the appearance of a folded monomer in mixed micelles of LPS and Triton X-100 in vitro (de Cock and Tommassen, 1996). A PhoE mutant was later shown to fold in vivo and also in vitro into LDAO micelles but not into mixed micelles of Triton X-100 and LPS, leading to further doubts about the existence of a folded monomeric intermediate of PhoE in LPS in vivo (Jansen et al., 2000). Folding and trimerization of OmpF (Surrey et al., 1996) was observed after interaction of urea-unfolded OmpF with preformed lipid bilayers in absence of detergent. Membrane inserted dimers of OmpF were detected transiently. In vitro, the folding yields of OmpF into lipid bilayers are small (<∼30%) even under optimized conditions (Surrey et al., 1996) and when compared to OmpA, which quantitatively folds at pH 10.

4. Electrophoretic mobility of OMPs depends on OMP structure

Most methods sensitive to structure and structural changes can be used to study the mechanistic principles of folding of β-barrel membrane proteins. A very simple and useful technique in folding studies on β-barrel membrane proteins is based on electrophoresis. The β-barrel structures of outer membrane proteins of bacteria are usually very stable and survive the treatment with the denaturing detergent SDS at room temperature. Native and denatured forms of many monomeric OMPs migrate at two different apparent molecular weights in sodium dodecyl sulfate polyacrylamide gel electrophoresis (SDS-PAGE) according to Laemmli (1970), if the samples are not boiled, i.e. denatured, prior to electrophoresis (*cold* SDS-PAGE). Folded monomers, dimers, and trimers can also be observed depending if the folded protein is a trimer (de Cock et al., 1996; Surrey et al., 1996). Natively folded monomers of OMPs migrate differently than unfolded OMPs, which is a consequence of the stability and more compact structure of the native β-barrels. For example, outer membrane protein A (OmpA) migrates at 35 kDa in denatured form and at 30 kDa in native form when isolated from membranes (Schweizer et al., 1978), the ferrichrome iron receptor FhuA migrates at 78 kDa in denatured form and at 54 kDa in non-denatured form and the major diffusion porin FomA of *Fusobacterium nucleatum* migrates at 40 kDa in unfolded form and at 37 kDa in non-denatured form (Puntervoll et al., 2002) as shown in Fig. 2. There are also OMPs where a difference in migration of folded and unfolded forms cannot be observed, such as the nucleoside specific porin Tsx, which in native form is not stable enough against unfolding by SDS at room temperature (Maier et al., 1988). The difference in migration of

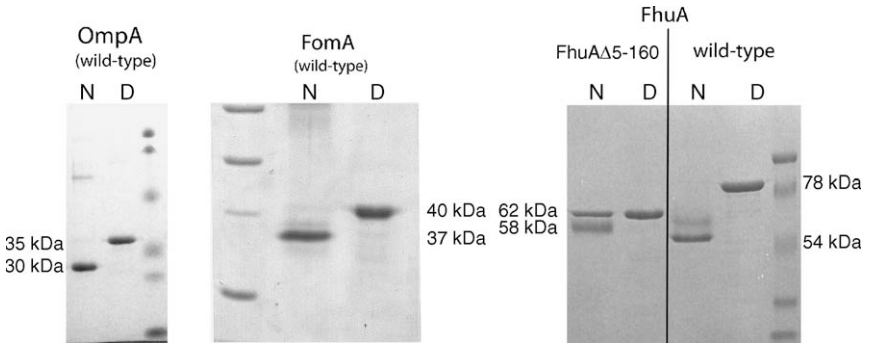

Fig. 2. Native and denatured forms of outer membrane proteins migrate differently on SDS-polyacrylamide gels, if samples are not denatured prior to electrophoresis. Here the different electrophoretic mobilities of native (N) and denatured (D) OMPs are shown for OmpA (N: 30 kDa, D: 35 kDa), FomA (N: 37 kDa, D: 40 kDa), FhuA△5-160 (N: 58 kDa, D: 62 kDa), and FhuA (N:54 kDa, D:78 kDa).

OMPs isolated in native form before and after unfolding can be used in folding studies, because it is expected that successful refolding of denatured OMPs, will also lead to a recovery of the electrophoretic mobility of the native protein. This has been observed for several outer membrane proteins, which were refolded to their native structure as observed by electrophoresis, before their high-resolution structure was solved either by X-ray crystallography or NMR-spectroscopy. Examples are the transmembrane domain of OmpA (Arora et al., 2001; Pautsch and Schulz, 1998; Pautsch et al., 1999) and the ferrienterobactin receptor FepA (Buchanan, 1999; Buchanan et al., 1999). In other cases, recovery of the electrophoretic mobility of the native protein by refolding corresponded always with spectroscopic results confirming formation of native structure and with assays demonstrating the functional activity of the refolded OMP. For example, for wild-type (WT) OmpA, all structural and functional experiments have shown identity between the 30 kDa form and structurally intact and fully functional OmpA. These previous studies included analysis of the OmpA structure by Raman (Vogel and Jähnig, 1986), FT-IR (Rodionova et al., 1995), and CD spectroscopy (Dornmair et al., 1990; Kleinschmidt et al., 1999b; Surrey and Jähnig, 1992, 1995), biochemical digestion experiments (Kleinschmidt and Tamm, 1996; Surrey and Jähnig, 1992), and functional assays such as phage inactivation (Schweizer et al., 1978), and single channel conductivity measurements (Arora et al., 2000). Similar observations were made for other OMPs, for example FomA (Pocanschi et al., 2006).

5. Folding kinetics of β-barrel membrane proteins determined by electrophoresis (KTSE)

The different migration of the folded form of an OMP, monitored by electrophoresis, can also be used to determine the kinetics of membrane protein folding as shown for the OmpA (Kleinschmidt and Tamm, 1996, 2002; Surrey and Jähnig, 1995), OmpG (Conlan and Bayley, 2003) and FomA (Pocanschi et al., 2006), and also for the trimer OmpF (Surrey et al., 1996) (kinetics of tertiary and quarternary structure formation by electrophoresis, KTSE). In this assay to determine folding kinetics, folding is initiated by strong dilution of the denaturant upon addition of preformed lipid bilayers or detergent micelles to unfolded OMP. SDS is then added to small volumes of the reaction mixture that are taken out at defined times after initiation of folding. In these samples, SDS binds quickly to both, folded and unfolded OMP and stops further OMP folding (Kleinschmidt and Tamm, 1996, 2002). SDS is not able to unfold already folded OMPs at room temperature. Finally, the fraction of folded OMP in all samples taken at the different times was determined by cold SDS-PAGE (i.e. without heat-denaturing the samples) and densitometric analyses of the bands of folded and of unfolded OMP, thus monitoring the kinetics of tertiary structure formation. For many OMPs, folding intermediates are usually not observed by electrophoresis, most probably because they are not stable enough to resist unfolding after addition of SDS or the electrical field applied in electrophoresis. An exception has been reported for OmpA, where an intermediate migrating at $M_{app} \approx 32$ kDa was observed transiently upon folding of urea-denatured OmpA into small unilamellar vesicles (SUVs) of dioleoyl phosphatidylcholine ($di C_{18:1}$PC) in the first 30 min of OmpA refolding at 30 °C (Kleinschmidt and Tamm, 1996). This intermediate was not observed at 20 or 40 °C or upon folding of OmpA into other phospholipids or detergents (Kleinschmidt and Tamm, 1996, 2002; Kleinschmidt et al., 1999b). It correlated with a partially inserted OmpA folding intermediate detected by fluorescence quenching with brominated lipids (Kleinschmidt et al., 1999a;

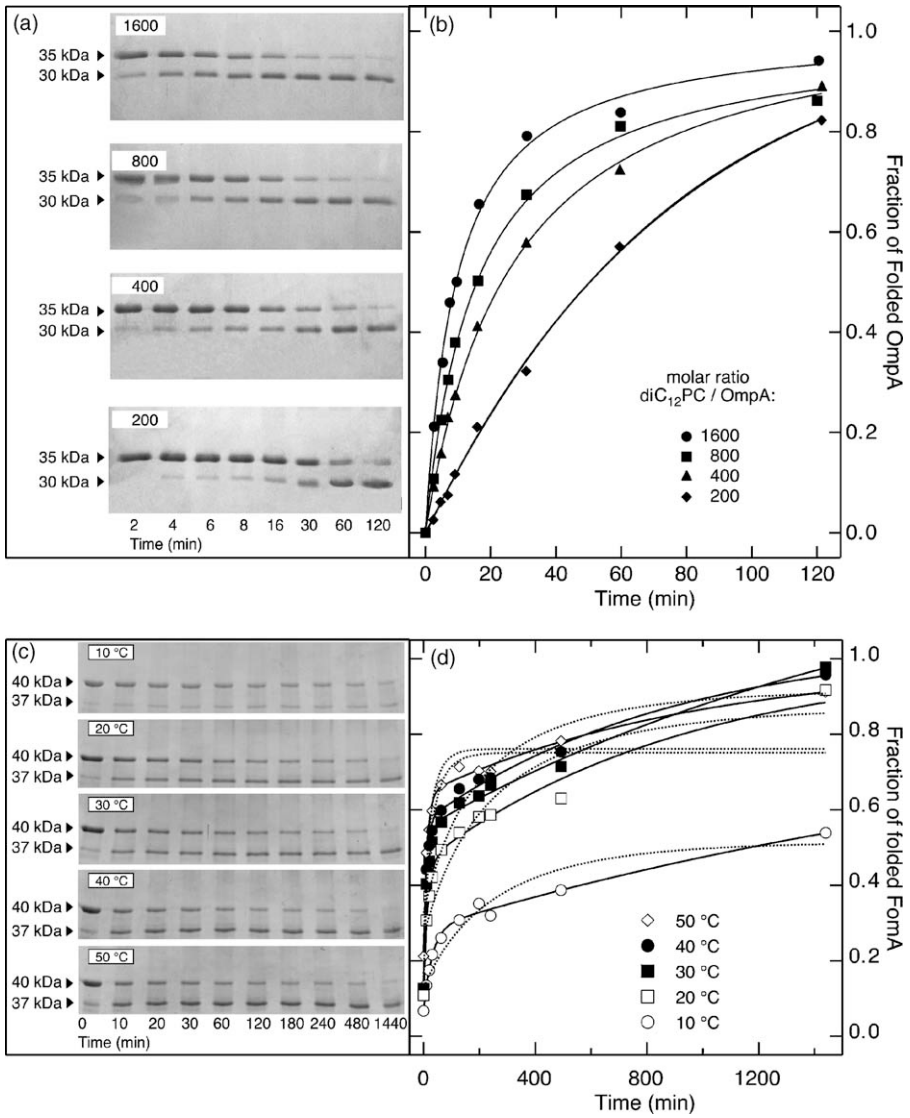

Fig. 3. Folding kinetics of OmpA and FomA into phospholipid bilayers measured by the KTSE method: (a) folding kinetics of OmpA (17.0 μM) folding into *di*C_{12}PC (LUVs, 100 nm diameter) analyzed by SDS-PAGE and measured by appearance of the 30 kDa folded form at the expense of the 35 kDa unfolded form of OmpA as a function of time. Experiments were performed at various molar ratios of Lipid/OmpA from 200 to 1600 and at 20 °C; (b) the fractions of folded OmpA determined by densitometry from the gels of panel (a) are plotted as a function of time and fitted to a single-step second-order rate law. Panels a and b were adapted from Ref. Kleinschmidt and Tamm (2002); (c) FomA (7 μM) folding kinetics into lipid bilayers of *di*$C_{10:0}$PC (SUVs) measured by appearance of the 37 kDa folded form at the expense of the unfolded 40 kDa form of FomA by SDS-PAGE at a molar lipid/FomA ratio of 1000. Experiments were performed between 10 and 50 °C. (d) The fraction of folded FomA was determined by densitometry from the unfolded and folded FomA bands in each lane of the gels of panel (c) and plotted as a function of time. The kinetics was fitted to double exponential functions (—). Alternatively, data for FomA insertion and folding into *di*$C_{18:1}$PC at 30 and at 40 °C were also fitted to a second-order rate law, assuming a single insertion and folding step (. . .) (Kleinschmidt and Tamm, 2002). Panels c and d were adapted from Ref. Pocanschi et al. (2006).

Kleinschmidt and Tamm, 1999) (I_{M3}, see below). Typically, only two bands of folded and unfolded forms of the OMP are detected as shown in Fig. 3 on the examples of OmpA (Fig. 3a) and FomA (Fig. 3c). The KTSE method therefore reports on the last folding step, leading to the native and thermodynamically stable OMP. Since only two bands are observed, it is expected that folding kinetics follow a single-step rate law and describe the last folding phase, i.e. folding intermediates are not detected. This has been demonstrated for OmpA, for which a single-step second-order rate law (pseudo-first-order at high lipid concentrations) described the

Table 2
Rate constants for the final folding step of OMPs by the KTSE method

Lipid	T[a] (°C)	$[P]$[b] (μM)	$[L]$[c] (mM)	k[d] (min^{-1})	$k_{F,2\,ord}$[e] ($min^{-1}\,M^{-1}$)	Yield
A. OmpA, described by a *single kinetic phase* (from Refs. Kleinschmidt and Tamm (1996, 2002))						
di$C_{12:0}$PC (L[f])	20	17	3.5	0.020	5.7	1.0
di$C_{12:0}$PC (L)	20	17	7.0	0.038	5.4	0.86
di$C_{12:0}$PC (L)	20	17	14.1	0.059	4.2	0.84
di$C_{12:0}$PC (L)	20	17	28.1	0.090	3.2	0.88
di$C_{18:1}$PC (S[f])	30	9	3.6	0.027	7.5	0.71
di$C_{18:1}$PC (S)	40	9	3.6	0.031	8.6	0.85

Lipid	T (°C)	$[P]$ (μM)	$[L]$ (mM)	A_F[g]	k_F[h] (min^{-1})	$k_{F,2\,ord}$[i] ($min^{-1}\,M^{-1}$)	A_S	k_S (min^{-1})	$k_{S,2\,ord}$ ($min^{-1}\,M^{-1}$)
B. FomA described by *two parallel kinetic phases* (from Ref. Pocanschi et al. (2006))									
di$C_{10:0}$PC (S)	50	7	7	0.55	0.082	11.7	0.45	0.00103	0.15
di$C_{10:0}$PC (S)	40	7	7	0.48	0.11	15.0	0.52	0.00113	0.16
di$C_{10:0}$PC (S)	30	7	7	0.34	0.086	12.3	0.66	0.00053	0.075
di$C_{10:0}$PC (S)	20	7	7	0.27	0.058	8.3	0.73	0.00038	0.054
di$C_{10:0}$PC (S)	10	7	7	0.26	0.032	4.6	0.74	0.00037	0.052
di$C_{18:1}$PC (S)	50	7	7	0.35	0.118	16.9	0.65	0.00062	0.089
di$C_{18:1}$PC (S)	40	7	7	0.17	0.059	8.4	0.83	0.00027	0.039
di$C_{18:1}$PC (S)	30	7	7	0.06	0.022	3.1	0.94	0.00009	0.013

The data from Refs. Kleinschmidt and Tamm (2002) and Pocanschi et al. (2006) were obtained at pH 10.0. data from Ref. Kleinschmidt and Tamm (1996) (OmpA folding into *di*$C_{18:1}$PC) were obtained at pH 8.5.

[a] Temperature.

[b] Protein concentration.

[c] Lipid concentration.

[d] Pseudo-first-order rate constants determined from the second-order rate constant and $[L]$.

[e] Second-order rate constant determined from fits to a second-order rate law.

[f] L: large unilamellar vesicles, S: small unilamellar vesicles.

[g] Relative contributions of each of the two kinetic phases (obtained by division of each preexponential fit parameter by the sum of the two preexponential fit parameters, see Eq. (2)).

[h] Pseudo-first-order rate constants determined from double exponential fits to Eq. (2).

[i] Lipid concentration-independent second-order rate constants (Kleinschmidt and Tamm, 2002), determined from the first-order rate constants by division by the lipid concentration, assuming pseudo-first-order kinetics for each phase.

observed kinetics of OmpA folding into bilayers of short-chain phospholipids, such as *di*$C_{12:0}$PC (Fig. 3b) (Kleinschmidt and Tamm, 2002) and into bilayers of *di*$C_{18:1}$PC (Kleinschmidt and Tamm, 1996) reasonably well, i.e. appearance of the folded form was described by

$$[P_F](t) = \frac{[P_U]_0[L]_0(\exp\{([P_U]_0 - [L]_0)k_{2\,ord}t\} - 1)}{[P_U]_0\,\exp\{([P_U]_0 - [L]_0)k_{2\,ord}t\} - [L]_0}, \quad (1)$$

where $[P_F](t)$ is the concentration of folded protein at time t, $k_{2\,ord}$ the second-order rate constant $[P_U]_0$, and $[L]_0$ are the initial concentrations of unfolded protein and the lipid (Kleinschmidt and Tamm, 2002). At larger lipid concentrations (L/P > ~100 mol/mol), fits by a *single-step* pseudo-first-order kinetics, i.e. simple mono-exponential kinetics, were sufficient to describe the folding kinetics of OmpA. OmpA folding kinetics into bilayers of short-chain phospholipids such as *di*$C_{12:0}$PC were not of true first-order, because the calculated first-order rate constants of OmpA folding increased with the lipid concentration (Table 2A). By contrast, fitting a second-order rate law to these kinetics resulted in rate constants that did not depend as strongly on the concentration of the phospholipid (Kleinschmidt and Tamm, 2002). Folding into *di*$C_{12:0}$PC was still successful with LUVs and at 20 °C. OmpA did not fold into LUVs of *di*$C_{18:1}$PC or into *di*$C_{14:0}$PC, but only into SUVs of these lipids and folding required a higher temperature, 30 or 40 °C.

6. Parallel pathways for OMP insertion and folding into lipid bilayers

KTSE experiments were also successfully performed with FomA of *Fusobacterium nucleatum* (Pocanschi et al., 2006), which is predicted to form a 14-stranded transmembrane β-barrel (Puntervoll et al., 2002) (Fig. 3, panels c and d). Unfolded FomA in 10 M urea folded

into LUVs and SUVs of *di*$C_{10:0}$PC and into SUVs of *di*$C_{18:1}$PC. Folding yields were higher and kinetics were faster into bilayers of *di*$C_{10:0}$PC (SUVs). Kinetics obtained from densitometric analyses of the SDS polyacrylamide gels (Fig. 3c) were strongly temperature dependent (Fig. 3d), as observed previously for OmpA (Kleinschmidt and Tamm, 1996). In contrast to folding kinetics of OmpA, the time courses of FomA folding into *di*$C_{10:0}$PC could not be fitted by a single-step rate law (dotted fit lines in Fig. 3c). FomA folding kinetics were fitted well by two pseudo-first-order kinetic phases, independent of the lipid used in FomA folding experiments. The non-linear least-square fits of double-exponential functions:

$$[P_F](t) = (A_1 + A_2)[A_0 + A_F \exp(k_F t) + A_S \exp(k_S t)], \quad (2)$$

to this data are shown in Fig. 3d (solid fit lines). In Eq. (2), $[P_F](t)$ is the concentration of the folded protein at time t, k_F and k_S are the rate constants of the fast and the slow kinetic phases and the pre-exponential factors $A_F = A_1/(A_1 + A_2)$ and $A_S = A_2/(A_1 + A_2)$, their relative contributions to the folding kinetics. The relative contributions and the calculated rate constants of the two observed kinetic phases of FomA insertion and folding are summarized in Table 2 for folding into *di*$C_{10:0}$PC and into *di*$C_{18:1}$PC. The fast and slow phase observed for formation of the folded form of FomA (migrating at 37 kDa) could only be explained by parallel folding phases, since no additional bands were observed on these gels (Pocanschi et al., 2006). The relative contributions and rate constants of the fast and slow phases of FomA folding into the two different lipid bilayers are summarized in Table 2B.

The halftimes $\tau_{1/2} = \ln(2)/k$ of FomA folding into *di*$C_{10:0}$PC (SUVs) ranged from ~22 min (at 10 °C) to ~7 min (at 40–50 °C) for the fast folding pathway and from ~1900 min (10 °C) to ~700 min (50 °C) for the slow folding pathway (Fig. 3c and d) (Pocanschi et al., 2006). Similarly, when FomA folding experiments were performed with *di*$C_{18:1}$PC (SUVs) instead of *di*$C_{10:0}$PC (Pocanschi et al., 2006), FomA folding was characterized by halftimes ranging from ~30 min (at 10 °C) to ~6 min (at 40–50 °C) for the fast folding pathway and from ~7800 min (10 °C) to ~1100 min (at 40–50 °C) for the slow pathway. Although the slow pathway of FomA folding may likely not be relevant for the integration of FomA into the outer membrane of a bacterium, this observation is important for two reasons. First, in the analysis of the rate of OMP insertion and folding into lipid bilayers, the rate of the faster process would be underestimated, if kinetic data were analyzed assuming only one folding pathway. The relative contribution of the slow pathway depended on the lipid bilayer and on temperature and was in between 45 and 94% (Table 1), strongly changing the total folding rate. Second, the knowledge of the existence of two pathways is important to study the effects of molecular chaperones on the folding of OMPs in model systems.

A possible explanation for the faster rate of folding into *di*$C_{10:0}$PC bilayers could be that the thinner bilayers are more flexible (Rawicz et al., 2000), supporting changes in protein conformation relative to the bilayer surface and therefore increasing the likelihood for insertion. It is possible that on a less flexible bilayer, a smaller fraction of the inserting FomA molecules would have the right orientation for insertion and folding along the fast pathway (Table 2). This interpretation would also be consistent with the temperature dependence of the relative contribution of the faster folding pathway, which is increased at higher temperatures, i.e. at higher flexibility of the bilayer. The rate constant of the faster process is not quite as strongly affected by bilayer thickness as the relative contribution of the fast folding process to the total rate of folding (Table 2).

7. Dependence of OMP insertion and folding on lipid bilayer properties

OmpA folding kinetics into lipid bilayers determined using the KTSE method depended on concentration of the lipid (Kleinschmidt and Tamm, 2002; Surrey and Jähnig, 1995), on the length of the lipid acyl chains (Kleinschmidt and Tamm, 2002), on the size of the lipid vesicles (Kleinschmidt and Tamm, 2002; Surrey and Jähnig, 1992), on the presence of a fluid phase of the lipid bilayer (Surrey and Jähnig, 1992), on temperature (Kleinschmidt and Tamm, 1996), and on pH (Surrey and Jähnig, 1995). OmpA folds into SUVs, but not into large unilamellar vesicles (LUVs) of *di*$C_{14:0}$PC (Surrey and Jähnig, 1992) and *di*$C_{18:1}$PC (Kleinschmidt and Tamm, 1996). OmpA will also fold into LUVs, if short-chain phospholipids of 12 or fewer carbons in the acyl chains are used in folding experiments (Kleinschmidt and Tamm, 2002).

8. pH- and lipid headgroup dependence of the folding of β-barrel membrane proteins

Although OmpA folded quantitatively into a wide range of neutral detergents, it did not fold into negatively charged SDS-micelles at neutral or basic pH (cf. Ref. Dornmair et al. (1990)). The negative charge of SDS

could not be the only reason for lack of folding into these micelles, since OmpA folded partially into micelles of negatively charged LPS at pH 7 (Bulieris et al., 2003) and also into bilayers containing negatively charged phosphatidylglycerol (Bulieris et al., 2003; Freudl et al., 1986). Surrey and Jähnig reported that OmpA folding yields reached 100% in neutral bilayers of *di*$C_{14:0}$PC at pH 10, but were only ~70% at neutral pH (Surrey and Jähnig, 1995). The increased folding yield at pH 10 was very likely a consequence of an increased negative surface charge of OmpA (p$I = 5.9$) at pH 10 that increased the solubility of OmpA, i.e. suppresses the aggregation side reaction. OmpA folding yields were again much lower at the even higher pH 12 (Surrey and Jähnig, 1995), which could be explained by deprotonation of the arginine side-chains of OmpA leading to a further increased negative net charge or negative surface potential of OmpA, which is then too high to allow structure formation. Charge–charge repulsions between the negative surface potential of SDS-micelles and negative charges on OmpA might also explain why OmpA did not fold into SDS micelles. The relatively small headgroup of SDS in comparison with the negatively charged LPS or phosphatidylglycerol causes a higher charge density on the surface of the SDS micelle, preventing insertion and folding of OmpA, which is negatively charged above pH 5.9.

9. Lipid acyl chain length dependence

The second-order rate constants strongly depended on the lengths of the acyl chains of the lipids. When OmpA folding into bilayers of *di*C_{12}PC was monitored by fluorescence spectroscopy, this rate constant was $k_{2\,ord} \approx 0.4\,l{\cdot}mol^{-1}{\cdot}s^{-1}$, while it was $k_{2\,ord} \approx 5.2\,l{\cdot}mol^{-1}{\cdot}s^{-1}$ for OmpA folding into bilayers of *di*$C_{11:0}$PC and $k_{2\,ord} \approx 30\,l{\cdot}mol^{-1}{\cdot}s^{-1}$ for OmpA folding into *di*$C_{10:0}$PC bilayers (Kleinschmidt and Tamm, 2002). The chain-length dependence for OmpA insertion and folding is consistent with the hydrophobic thickness of most outer membrane proteins of known crystal structure, which is in the range of 22–25 Å determined from available OMP crystal structures, for a review, see Ref. Lee (2003). The hydrophobic thickness of lipid bilayers of *di*$C_{12:0}$PC in the fluid phase was determined to 19.5 ± 1 Å (Lewis and Engelman, 1983), suggesting that fluid *di*C_{12}PC bilayers would provide a better hydrophobic matching to outer membrane proteins than fluid *di*$C_{18:1}$PC (27 ± 1 Å), because the chains of *di*$C_{10:0}$PC may be stretched in the vicinity of TMPs with longer hydrophobic length (de Planque et al., 1998), for reviews see Refs. Killian (1998) and Marsh (1990). The energy requirement for bilayer thickening is small up to the limit of full extension of the acyl chains. The energy cost of a 33% increase in bilayer thickness, which corresponds to a ~25% reduction of the molecular surface area, was determined to only about 2 kT per molecule (Lis et al., 1982; Parsegian et al., 1979). Membrane thinning may not occur as readily as membrane thickening, because even 2–3% surface area increases destabilized the bilayer structure and broke membranes (Kwok and Evans, 1981). However, it may be that insertion and folding of OMPs do not depend on hydrophobic matching, but instead on other lipid bilayer properties that are lipid chain-length dependent. Insertion and folding may depend on bilayer flexibility and surface curvature stress and therefore indirectly on lipid chain length. A more flexible bilayer might support conformational changes of surface adsorbed folding intermediates that lead to insertion and folding.

10. Synchronized kinetics of secondary and tertiary structure formation of the β-barrel of OmpA

The kinetics of folding of OmpA into lipid bilayers can also be determined by circular dichroism (CD) spectroscopy (Kleinschmidt and Tamm, 2002). When the folding kinetics were measured for OmpA folding into LUVs of saturated short-chain phospholipids, a similar dependence of the rate constants on the length of the hydrophobic acyl chains of the lipids was observed as by fluorescence spectroscopy and by KTSE. Secondary structure formation was fastest with *di*$C_{10:0}$PC (LUVs) and slowest with *di*$C_{12:0}$PC (LUVs) as determined from the circular dichroism kinetics at 204 nm. When OmpA was reacted with preformed lipid bilayers (LUVs) of *di*$C_{14:0}$PC or *di*$C_{18:1}$PC, no changes were observed in the CD signals, indicating no changes in the secondary structure of OmpA. The rate constants observed by circular dichroism spectroscopy were very similar to the rate constants of OmpA folding observed by KTSE assays listed in Table 2. For folding into LUVs of *di*$C_{12:0}$PC, the second-order rate constant obtained from the circular dichroism kinetics was $5.3\,l\,mol^{-1}\,min^{-1}$ at 20 °C, as averaged from four kinetic experiments at different lipid concentrations (Kleinschmidt and Tamm, 2002).

11. Interaction of OmpA with the lipid bilayer is faster than formation of folded OmpA

The rate constants of the secondary and tertiary structure formation of OmpA in *di*$C_{12:0}$PC were both ${}^{s/t}k_{2\,ord} \approx 5.3\,l\,mol^{-1}\,min^{-1} = 0.09\,l{\cdot}mol^{-1}{\cdot}s^{-1}$. By con-

trast, the second-order rate constant obtained from the fluorescence time courses of the OmpA folding kinetics into this lipid was about four- to five-fold higher ($^{pla}k_{2\,ord} \approx 0.4\,l{\cdot}mol^{-1}{\cdot}s^{-1}$), indicating that the adsorption and insertion of the fluorescent tryptophan residues of OmpA into the hydrophobic core of the lipid bilayer were faster than the formation of the fully folded form of OmpA. Four of the five tryptophans of OmpA are at the front end of the β-barrel and presumably interacted first with the hydrophobic core of the membrane, leading to fast fluorescence kinetics compared to the circular dichroism kinetics and kinetics of tertiary structure formation by electrophoresis. Together, these results indicated that the formation of the β-strands and the formation of the β-barrel of OmpA take place in parallel and are a consequence of the insertion of the membrane protein into the lipid bilayer. The previous observation that a preformed supramolecular assembly of amphiphiles is necessary for structure formation in OmpA was therefore further detailed by a kinetic characterization of the faster rates of interaction of OmpA with the lipid bilayer and by the slower rates of secondary and tertiary structure formation in OmpA.

12. Fluorescence time courses of OmpA folding into SUVs of *di*$C_{18:1}$PC indicate folding intermediates

Experiments with urea-unfolded OmpA and lipid membranes of *di*$C_{14:0}$PC indicated that OmpA folds into lipid bilayers of small unilamellar vesicles (SUVs) prepared by sonication, but not into bilayers of LUVs with a diameter of 100 nm prepared by extrusion (Surrey and Jähnig, 1992, 1995). Lipids with longer chains such as *di*$C_{14:0}$PC and *di*$C_{18:1}$PC required the preparation of SUVs by ultrasonication and temperatures greater than ∼25–28 °C for successful OmpA insertion and folding (Kleinschmidt and Tamm, 1996; Surrey and Jähnig, 1992).

Lipid bilayers of SUVs have a high surface curvature and intrinsic curvature stress. This leads to an increase of the hydrophobic surface that is exposed to OmpA after it is adsorbed at the membrane water interface, facilitating insertion of OmpA into SUVs compared to insertion of OmpA into bilayers of LUVs, where curvature stress is much lower and no insertion was observed. The folding kinetics of OmpA into SUVs of *di*$C_{14:0}$PC or *di*$C_{18:1}$PC were slower compared to the folding kinetics into LUVs short chain phospholipids and strongly temperature dependent (Kleinschmidt and Tamm, 2002). The fluorescence kinetics of OmpA folding that could still be fitted to a single-step pseudo-first-order rate law at 40 °C (Kleinschmidt and Tamm, 1996, 2002) were more complex when the temperature for folding was 30 °C or less. A single-step rate law was not sufficient to describe the kinetics (Kleinschmidt and Tamm, 1996). Insertion and folding of OmpA into bilayers of *di*$C_{18:1}$PC (SUVs) was characterized by at least three kinetic phases, when experiments were performed at temperatures between 2 and 40 °C. These phases could be approximated by pseudo-first order kinetics at a lipid/protein ratio of 400. Two folding steps could be distinguished by monitoring the fluorescence time courses at 30 °C. The first (faster) step was only weakly temperature dependent ($k_1 = 0.16\,min^{-1}$, at 0.5 mM lipid). The second step was up to two orders of magnitude slower at low temperatures, but the rate constant approached the rate constant of the first step at higher temperatures (∼$0.0058\,min^{-1}$ at 2 °C and ∼$0.048–0.14\,min^{-1}$ at 40 °C, in presence of 0.5 mM lipid). The activation energy for the slower process was 46 ± 4 kJ/mol (Kleinschmidt and Tamm, 1996). An even slower phase of OmpA folding was observed by KTSE assays, indicating that tertiary structure formation was slowest with a rate constant $k_3 = 0.9 \times 10^{-2}\,min^{-1}$ (at 3.6 mM lipid and at 40 °C) (Kleinschmidt and Tamm, 1996). This is consistent with the smaller rate constants of secondary and tertiary structure formation in comparison to the rate constants of protein association with the lipid bilayer, which were later observed for OmpA folding into LUVs of short-chain phospholipids (Kleinschmidt and Tamm, 2002). The kinetic phases that were observed for OmpA folding into *di*$C_{18:1}$PC bilayers (SUVs) suggest that at least two membrane-bound OmpA folding intermediates exist when OmpA folds and inserts into lipid bilayers with 14 or more carbons in the hydrophobic acyl chains. These membrane-bound intermediates could be stabilized in fluid *di*$C_{18:1}$PC bilayers at low temperatures between 2 and 25 °C (the temperature for the phase-transition of *di*$C_{18:1}$PC from the lamellar-ordered to the lamellar-disordered, liquid crystalline phase is $T_c = -18$ °C). The low-temperature intermediates could be rapidly converted to fully inserted, native OmpA, as demonstrated by temperature jump experiments (Kleinschmidt and Tamm, 1996).

13. Characterization of folding intermediates by fluorescence quenching

Tryptophan fluorescence quenching by brominated phospholipids (Alvis et al., 2003; Bolen and Holloway, 1990; Everett et al., 1986; Ladokhin, 1999a, 1999b; Ladokhin and Holloway, 1995; Markello et al., 1985; Williamson et al., 2002) or by lipid spin-labels (Abrams and London, 1992, 1993; Cruz et al., 1998; Fastenberg

et al., 2003; Piknova et al., 1997; Prieto et al., 1994) has been very valuable to determine characteristic elements of the transmembrane topology and lipid–protein interactions of integral membrane proteins. To further characterize the folding process of OmpA, we combined this method with the study of the folding kinetics of OmpA into bilayers (SUVs) of *di*$C_{18:1}$PC (Kleinschmidt et al., 1999a; Kleinschmidt and Tamm, 1999). The average positions of the five fluorescent tryptophans of OmpA were characterized for the membrane-bound folding intermediates that were previously implicated by the discovery of multi-step folding kinetics (Kleinschmidt and Tamm, 1996). A new method was developed by studying the kinetics of the refolding process in combination with the tryptophan fluorescence quenching at different depths in the lipid bilayer (Kleinschmidt and Tamm, 1999) using membrane embedded quenchers. The positions of fluorescent tryptophans with reference to the center of the phospholipid bilayer can be determined using a set of membrane integrated fluorescence quenchers that carry either two vicinal bromines or alternatively a doxyl group in the *sn*-2 acyl chain of the phospholipid. When in close proximity to the fluorescent tryptophan residues of integral membrane proteins, these groups quench the tryptophan fluorescence. The positions of the bromines in 1-palmitoyl-2-(4,5-dibromo-)stearoyl-*sn*-glycero-3-phosphocholine (4,5-DiBrPC), in 6,7-DiBrPC, in 9,10-DiBrPC, and in 11,12-DiBrPC are known from X-ray diffraction to be 12.8, 11.0, 8.3, and 6.5 Å from the center of the lipid bilayer (McIntosh and Holloway, 1987; Wiener and White, 1991). The fluorescence intensity of the tryptophans of OmpA was measured as a function of time after initiation of OmpA folding by dilution of the denaturant in presence of preformed lipid bilayers containing one of the brominated lipids as a fluorescence quencher. In a set of four equivalent folding experiments, bilayers were used that contained 30 mol% of one of the four brominated lipids and 70% *di*$C_{18:1}$PC. The fluorescence intensities in the four different time courses of OmpA folding in presence of each of the four brominated lipids were subsequently normalized by division with fluorescence intensities obtained upon OmpA folding into bilayers of 100% *di*$C_{18:1}$PC (i.e. in absence of any quencher). Thus, depth-dependent quenching profiles were obtained at each time after initiation of OmpA folding. From these profiles, the vertical location of Trp in the membrane in projection to the bilayer normal was then determined using the distribution analysis (Ladokhin, 1999a; Ladokhin and Holloway, 1995) or the parallax method (Abrams and London, 1992; Chattopadhyay and London, 1987).

A large set of experiments was performed in the temperature range between 2 and 40 °C. At each selected temperature, the average distances of the tryptophans to the center of the lipid bilayer were determined as a function of time. Therefore, we called this method time-resolved distance determinations by tryptophan fluorescence quenching (TDFQ) (Kleinschmidt and Tamm, 1999). Previously unidentified folding intermediates on the pathway of OmpA insertion and folding into lipid bilayers were detected, trapped and characterized. Three membrane-bound intermediates were described, in which the average distances of the Trps from the bilayer center were 14–16 Å (I_{M1}), 10–11 Å (I_{M2}), and 0–5 Å (I_{M3}), respectively (Kleinschmidt and Tamm, 1999). The first folding intermediate was stable at 2 °C for at least 1 h. The second intermediate was characterized at temperatures between 7 and 20 °C. The Trps moved 4–5 Å closer to the center of the bilayer at this stage. Subsequently, in the third intermediate that was observed at 26–28 °C, the Trps moved another 5–11 Å closer to the center of the bilayer. This intermediate appeared to be less stable. The distribution parameter *s*, calculated from distribution analysis, was largest for the Trp distribution of this intermediate. This was a consequence of the mechanism of folding and of the structure of folded OmpA (Arora et al., 2001; Pautsch and Schulz, 1998, 2000). The large distribution parameter observed for this intermediate was consistent with experiments on single Trp mutants of OmpA (Kleinschmidt et al., 1999a) (see below). Trp-7 has to remain in the first leaflet of the lipid bilayer, while the other Trps must be translocated across the bilayer to the second leaflet. Therefore, with symmetrically incorporated brominated lipids as fluorescence quenchers, the largest distribution parameter was observed when the four translocating Trps are in the center of the lipid bilayer. Formation of the native structure of OmpA was observed at temperatures >∼28 °C. In the end of these kinetic experiments, all five Trps were finally located on average about 9–10 Å from the bilayer center, Trp-7 in the periplasmic leaflet and the other four Trps in the outer leaflet of the outer membrane.

When KTSE experiments were performed to monitor OmpA folding at 30 °C, a 32 kDa band was observed in the first few minutes of OmpA folding (Kleinschmidt and Tamm, 1996). The folding conditions for this experiment were nearly identical to those of the fluorescence quenching experiments at 28–30 °C. Therefore, this 32 kDa form is very likely identical to the third folding intermediate of OmpA (I_{M3}), in which the average Trp-location is 0–5 Å from the center of the lipid bilayer. The comparison indicated that in this intermediate, a significant

part of the β-barrel had formed, which is resistant to treatment with SDS at room temperature.

14. The β-barrel domain of OmpA folds and inserts by a concerted mechanism

TDFQ experiments were subsequently performed with the five different single Tryptophan mutants of OmpA. These mutants were prepared by site-directed mutagenesis (Kleinschmidt et al., 1999a), and contained each a single tryptophan and four phenylalanines in the five tryptophan positions of the wild-type protein. All mutants were isolated from the *E. coli* outer membrane and refolded in vitro into lipid bilayers. Time-resolved distance determinations (TDFQ) for each of the single Trp mutants of OmpA gave more structural detail on the folding mechanism of OmpA. TDFQ experiments were carried out at selected temperatures between 2 and 40 °C (Kleinschmidt et al., 1999a). When kinetic experiments were performed below 30 °C, each of the five tryptophans approached a distance of 10–11 Å from the bilayer center in the end of the fluorescence time course of OmpA folding. The distance decrease with time was observed even at 40 °C for Trp-7 (Fig. 4a). The TDFQ results showed that Trp-7 did not migrate any closer to the bilayer center than ∼10 Å independent of the experimental conditions. However, Trp-15, Trp-57, Trp-102, and Trp-143, were detected very close to the center of the lipid bilayer in the first minutes of refolding at temperatures of 30, 32, 35, and 40 °C, respectively. This is shown for Trp-143 in Fig. 4b. TDFQ experiments performed at 40 °C resolved the last two steps of OmpA refolding and the translocation rate constants of the first phase of fast distance change were 0.55, 0.46, 0.26, and 0.43 min^{-1} for Trp-15, Trp-57, Trp-102, and Trp-143, respectively. The four Trps crossed the center of the bilayer and approached distances of ∼10 Å from the bilayers center in the final folding step of OmpA. These experiments demonstrated that Trp-15, Trp-57, Trp-102, and Trp-143 are similarly located in three folding intermediates that were also observed previously for wild-type OmpA. The similar distances of these Trps from the membrane center in each of the membrane-bound folding intermediates indicate a simultaneous translocation of the transmembrane segments of OmpA, coupled to the formation of the β-barrel structure upon insertion.

The results of these kinetic studies on the folding mechanism of OmpA may be used to develop a tentative model of OmpA folding (Fig. 5): The time courses of OmpA folding into phospholipid bilayers (LUVs) of *di*$C_{12:0}$PC indicated that β-strand secondary and β-barrel tertiary structure formation are synchronized with the same rate constant (Kleinschmidt and Tamm, 2002), which is lower than the rate constant of the fluorescence time course of OmpA adsorption to the lipid bilayer. Strongly temperature dependent kinetics were observed and several kinetic phases were distinguished, when folding of OmpA was investigated with lipid bilayers of *di*$C_{18:1}$PC, which is a phospholipid with comparably long hydrophobic chains. OmpA first adsorbs to the water–membrane interface (intermediate I_{M1}) and the intrinsic fluorescence of OmpA increases strongly due to the partitioning of the fluorescent Trps into the less polar environment at the membrane/water interface. Subsequently, the slower phase of the fluorescence changes reflect the migration of the Trps from the membrane/water interface into the hydrophobic core of the lipid bilayer. The translocation of the Trps across the bilayer is best monitored with membrane inserted fluorescence quenchers, since the intrinsic Trp fluorescence does not change much during Trp migration through the 30 Å hydrophobic core of *di*$C_{18:1}$PC. The average location of the Trps of 14–16 Å from the bilayer center after adsorption to the membrane–water interface was determined by TDFQ experiments at 2 °C (Kleinschmidt and Tamm, 1999). At temperatures of 5–25 °C, this initial phase of folding was fast and followed by a second, slower phase, in which the Trps move into more hydrophobic regions at a distance of about 10 Å from the bilayer center. The obserserved folding intermediate (I_{M2}) is quite stable. A third membrane-bound intermediate (I_{M3}) was identified at 27–29 °C. In this intermediate, all Trps, except Trp-7, are detected a distance of 0–5 Å from the bilayers center in the first minutes of OmpA folding. Trp-7 remains at the same location as in intermediate B. Very likely, this intermediate is identical to the 32 kDa form of OmpA that was previously observed by KTSE experiments (Kleinschmidt and Tamm, 1996). Finally, at temperatures above 28–30 °C, Trp-15, Trp-57, Trp-102, and Trp-143 move away from the center of the bilayer to a distance of about 10 Å. This distance of the Trp residues of OmpA compares well with the X-ray and NMR structures of OmpA (Arora et al., 2001; Pautsch and Schulz, 2000). The basic elements of the model in Fig. 5 are the synchronized kinetics of secondary and tertiary structure formation, the simultaneous migration of the tryptophans that cross the bilayer center, and the migration of Trp-7, which does not translocate. However, more structural information is needed to improve this preliminary model. For example, it is not known, how the residues of the polar loops of OmpA cross the hydrophobic core of the lipid bilayer.

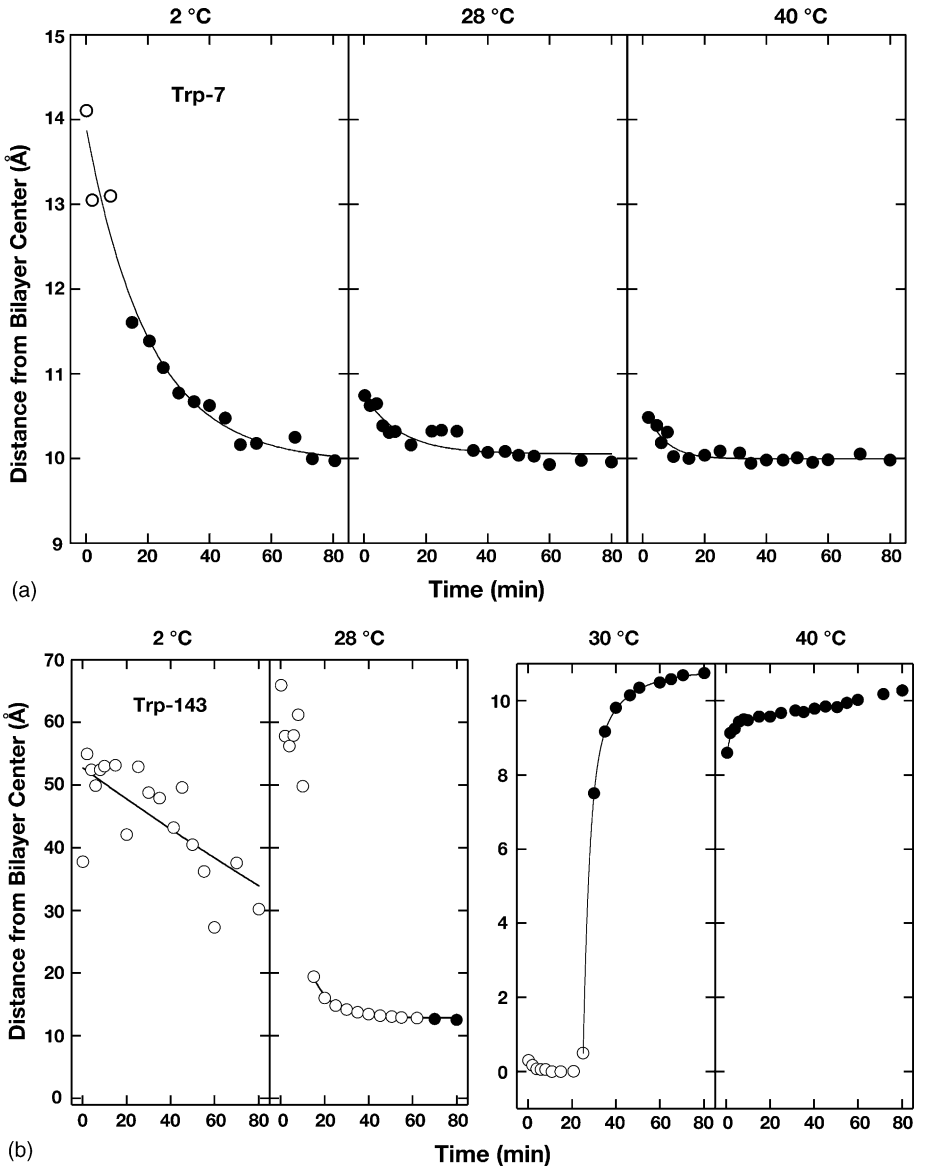

Fig. 4. (a) Time courses of the movement of Trp-7 towards the bilayer center at 2, 28, and 40 °C. Distances were obtained from curve fits to fluorescence quenching profiles as described in the text. Data points represented by closed circles were the fitted quenching profile minima, open circles denote extrapolated distances form the observed quenching profiles. The solid lines are fits of the data to single or double exponential functions. (b) Time courses of the movement of Trp-143 towards the bilayer center at 2 and 28 °C and from the bilayer center at 30 and 40 °C. At 2 °C, the distances of Trp-143 could only be obtained by extrapolation (open circles). The solid lines are fits of the data to single or double exponential functions. Figure adapted from Ref. Kleinschmidt et al. (1999a).

15. Perspectives

Exploration of insertion and folding of β-barrel membrane proteins into membranes has made progress in recent years, but our understanding of the process is still limited. The discovery of outer membrane protein targeting and/or folding machineries that exists in the periplasm and apparently also in the outer membrane (Doerrler and Raetz, 2005; Johnson and Jensen, 2004; Voulhoux et al., 2003; Werner and Misra, 2005) has raised new questions. While Skp (Bulieris et al., 2003; Chen and Henning, 1996) and SurA (Lazar and Kolter, 1996; Rouviere and Gross, 1996) were demonstrated to improve membrane insertion and folding of OmpA in vitro, these chaperones had no significant effects on the insertion and folding of some other outer membrane

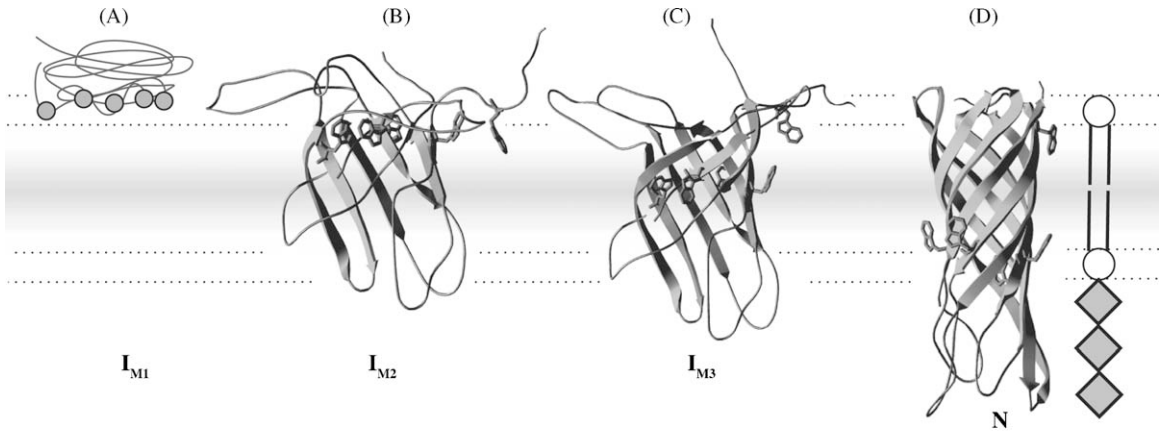

Locations of the Tryptophans of OmpA in Folding Intermediates identified by TDFQ:

Distance to the Center of the Lipid Bilayer

Tryptophan	I_{M1} →	I_{M2} →	I_{M3} →	N
⑦	~14-16 Å	~10 Å	~10 Å	~10 Å
15, 57, 102, 143		~10 Å	~0-5 Å	~10 Å

Fig. 5. Folding model of OmpA. The kinetics of β-sheet secondary and β-barrel tertiary structure formation in OmpA have the same rate constants and are coupled to the insertion of OmpA into the lipid bilayer (Kleinschmidt et al., 1999a; Kleinschmidt and Tamm, 1999, 2002). The locations of the five trpyptophans in the three identified membrane-bound folding intermediates and in the completely refolded state of OmpA (Kleinschmidt et al., 1999a; Kleinschmidt and Tamm, 1999) are shown. Additional details, such as the translocation of the long polar loops across the lipid bilayer must still be determined. OmpA structures were generated with DeepView (Guex and Peitsch, 1997; Schwede et al., 2003).

proteins into preformed lipid bilayers. It will be interesting, which additional chaperones will be discovered that assist the OMP assembly process in well-defined in vitro experiments. It will then be necessary to investigate whether these proteins are directly involved in the generation of structure in OMPs or whether they are key elements for the targeting of OMPs to the surface of the outer membrane, where OMP insertion into the phospholipid bilayer is then mediated by lipid-protein interactions. Some outer membrane proteins, for example OmpA, do not absolutely require folding machinery for quantitative folding in vitro from a urea-denatured state. However, in vivo, i.e. in absence of urea, chaperones such as Skp must prevent the hydrophobic collapse and misfolding of OMPs and deliver them to the outer membrane. In case of OmpA, insertion and folding appear to be driven by the interaction of a chaperone–OmpA complex with the lipid bilayer and apparently can take place in absence of membrane integrated proteins that act as folding machinery (Bulieris et al., 2003). The folding kinetics of OmpA in vitro depended a lot on the lipid bilayer properties. These properties may be modulated by peripherally bound or by intrinsic membrane proteins. Skp for example, is highly basic and may modulate the surface properties of the periplasmic leaflet of the outer membrane, which contains phosphatidylglycerol that is negatively charged. Future studies on the insertion and folding of β-barrel membrane proteins must therefore also include investigations, whether periplasmic proteins modify the properties of a lipid bilayer by binding to the bilayer surface. In addition, more detailed information must be obtained on the structure formation in OMPs. For example, it is not clear how the polar loops of the OMPs translocate across the hydrophobic core of the bilayer and which are the roles lipid–protein and protein–protein interactions have in this context.

Acknowledgements

The work from the laboratory of the author was supported by DFG grants KL 1024/2-5, KL 1024/2-6 and KL-1024/4-1.

References

Abrams, F.S., London, E., 1992. Calibration of the parallax fluorescence quenching method for determination of membrane penetration depth: refinement and comparison of quenching by spin-labeled and brominated lipids. Biochemistry 31, 5312–5322.

Abrams, F.S., London, E., 1993. Extension of the parallax analysis of membrane penetration depth to the polar region of model mem-

branes: use of fluorescence quenching by a spin-label attached to the phospholipid polar headgroup. Biochemistry 32, 10826–10831.

Ahn, V.E., Lo, E.I., Engel, C.K., Chen, L., Hwang, P.M., Kay, L.E., Bishop, R.E., Prive, G.G., 2004. A hydrocarbon ruler measures palmitate in the enzymatic acylation of endotoxin. EMBO J. 23, 2931–2941.

Alvis, S.J., Williamson, I.M., East, J.M., Lee, A.G., 2003. Interactions of anionic phospholipids and phosphatidylethanolamine with the potassium channel KcsA. Biophys. J. 85, 3828–3838.

Anfinsen, C.B., 1973. Principles that govern the folding of protein chains. Science 181, 223–230.

Arora, A., Abildgaard, F., Bushweller, J.H., Tamm, L.K., 2001. Structure of outer membrane protein A transmembrane domain by NMR spectroscopy. Nat. Struct. Biol. 8, 334–338.

Arora, A., Rinehart, D., Szabo, G., Tamm, L.K., 2000. Refolded outer membrane protein A of *Escherichia coli* forms ion channels with two conductance states in planar lipid bilayers. J. Biol. Chem. 275, 1594–1600.

Bolen, E.J., Holloway, P.W., 1990. Quenching of tryptophan fluorescence by brominated phospholipid. Biochemistry 29, 9638–9643.

Buchanan, S.K., 1999. Overexpression and refolding of an 80-kDa iron transporter from the outer membrane of *Escherichia coli*. Biochem. Soc. Trans. 27, 903–908.

Buchanan, S.K., Smith, B.S., Venkatramani, L., Xia, D., Esser, L., Palnitkar, M., Chakraborty, R., van der Helm, D., Deisenhofer, J., 1999. Crystal structure of the outer membrane active transporter FepA from *Escherichia coli*. Nat. Struct. Biol. 6, 56–63.

Bulieris, P.V., Behrens, S., Holst, O., Kleinschmidt, J.H., 2003. Folding and insertion of the outer membrane protein OmpA is assisted by the chaperone Skp and by lipopolysaccharide. J. Biol. Chem. 278, 9092–9099.

Chattopadhyay, A., London, E., 1987. Parallax method for direct measurement of membrane penetration depth utilizing fluorescence quenching by spin-labeled phospholipids. Biochemistry 26, 39–45.

Chen, R., Henning, U., 1996. A periplasmic protein (Skp) of *Escherichia coli* selectively binds a class of outer membrane proteins. Mol. Microbiol. 19, 1287–1294.

Chimento, D.P., Mohanty, A.K., Kadner, R.J., Wiener, M.C., 2003. Substrate-induced transmembrane signaling in the cobalamin transporter BtuB. Nat. Struct. Biol. 10, 394–401.

Cobessi, D., Celia, H., Folschweiller, N., Schalk, I.J., Abdallah, M.A., Pattus, F., 2005. The crystal structure of the pyoverdine outer membrane receptor FpvA from *Pseudomonas aeruginosa* at 3.6 Å resolution. J. Mol. Biol. 347, 121–134.

Conlan, S., Bayley, H., 2003. Folding of a monomeric porin, OmpG, in detergent solution. Biochemistry 42, 9453–9465.

Cowan, S.W., Schirmer, T., Rummel, G., Steiert, M., Ghosh, R., Pauptit, R.A., Jansonius, J.N., Rosenbusch, J.P., 1992. Crystal structures explain functional properties of two *E. coli* porins. Nature 358, 727–733.

Cruz, A., Casals, C., Plasencia, I., Marsh, D., Perez-Gil, J., 1998. Depth profiles of pulmonary surfactant protein B in phosphatidylcholine bilayers, studied by fluorescence and electron spin resonance spectroscopy. Biochemistry 37, 9488–9496.

de Cock, H., Tommassen, J., 1996. Lipopolysaccharides and divalent cations are involved in the formation of an assembly-competent intermediate of outer-membrane protein PhoE of *E. coli*. EMBO J. 15, 5567–5573.

de Cock, H., van Blokland, S., Tommassen, J., 1996. In vitro insertion and assembly of outer membrane protein PhoE of *Escherichia coli* K-12 into the outer membrane. Role of Triton X-100. J. Biol. Chem. 271, 12885–12890.

de Planque, M.R., Greathouse, D.V., Koeppe II, R.E., Schafer, H., Marsh, D., Killian, J.A., 1998. Influence of lipid/peptide hydrophobic mismatch on the thickness of diacylphosphatidylcholine bilayers. A ^{2}H NMR and ESR study using designed transmembrane α-helical peptides and gramicidin A. Biochemistry 37, 9333–9345.

Delano, W.L., 2002. The PyMOL Molecular Graphics System. DeLano Scientific, San Carlos, CA, USA.

Doerrler, W.T., Raetz, C.R., 2005. Loss of outer membrane proteins without inhibition of lipid export in an *Escherichia coli* YaeT mutant. J. Biol. Chem. 280, 27679–27687.

Dornmair, K., Kiefer, H., Jähnig, F., 1990. Refolding of an integral membrane protein, OmpA of *Escherichia coli*. J. Biol. Chem. 265, 18907–18911.

Dutzler, R., Rummel, G., Alberti, S., Hernandez-Alles, S., Phale, P., Rosenbusch, J., Benedi, V., Schirmer, T., 1999. Crystal structure and functional characterization of OmpK36, the osmoporin of *Klebsiella pneumoniae*. Struct. Fold. Des. 7, 425–434.

Everett, J., Zlotnick, A., Tennyson, J., Holloway, P.W., 1986. Fluorescence quenching of cytochrome b5 in vesicles with an asymmetric transbilayer distribution of brominated phosphatidylcholine. J. Biol. Chem. 261, 6725–6729.

Faller, M., Niederweis, M., Schulz, G.E., 2004. The structure of a mycobacterial outer-membrane channel. Science 303, 1189–1192.

Fastenberg, M.E., Shogomori, H., Xu, X., Brown, D.A., London, E., 2003. Exclusion of a transmembrane-type peptide from ordered-lipid domains (rafts) detected by fluorescence quenching: extension of quenching analysis to account for the effects of domain size and domain boundaries. Biochemistry 42, 12376–12390.

Ferguson, A.D., Chakraborty, R., Smith, B.S., Esser, L., van der Helm, D., Deisenhofer, J., 2002. Structural basis of gating by the outer membrane transporter FecA. Science 295, 1715–1719.

Ferguson, A.D., Hofmann, E., Coulton, J.W., Diederichs, K., Welte, W., 1998. Siderophore-mediated iron transport: crystal structure of FhuA with bound lipopolysaccharide. Science 282, 2215–2220.

Fernandez, C., Hilty, C., Wider, G., Guntert, P., Wüthrich, K., 2004. NMR structure of the integral membrane protein OmpX. J. Mol. Biol. 336, 1211–1221.

Forst, D., Welte, W., Wacker, T., Diederichs, K., 1998. Structure of the sucrose-specific porin ScrY from *Salmonella typhimurium* and its complex with sucrose. Nat. Struct. Biol. 5, 37–46.

Freudl, R., Schwarz, H., Stierhof, Y.D., Gamon, K., Hindennach, I., Henning, U., 1986. An outer membrane protein (OmpA) of *Escherichia coli* K-12 undergoes a conformational change during export. J. Biol. Chem. 261, 11355–11361.

Guex, N., Peitsch, M.C., 1997. SWISS-MODEL and the Swiss-PdbViewer: an environment for comparative protein modeling. Electrophoresis 18, 2714–2723.

Heins, L., Mentzel, H., Schmid, A., Benz, R., Schmitz, U.K., 1994. Biochemical, molecular, and functional characterization of porin isoforms from potato mitochondria. J. Biol. Chem. 269, 26402–26410.

Hong, H., Tamm, L.K., 2004. Elastic coupling of integral membrane protein stability to lipid bilayer forces. Proc. Natl. Acad. Sci. U.S.A. 101, 4065–4070.

Huang, K.S., Bayley, H., Liao, M.J., London, E., Khorana, H.G., 1981. Refolding of an integral membrane protein. Denaturation, renaturation, and reconstitution of intact bacteriorhodopsin and two proteolytic fragments. J. Biol. Chem. 256, 3802–3809.

Hwang, P.M., Choy, W.Y., Lo, E.I., Chen, L., Forman-Kay, J.D., Raetz, C.R., Prive, G.G., Bishop, R.E., Kay, L.E., 2002. Solution structure and dynamics of the outer membrane enzyme PagP by NMR. Proc. Natl. Acad. Sci. U.S.A. 99, 13560–13565.

Jansen, C., Heutink, M., Tommassen, J., de Cock, H., 2000. The assembly pathway of outer membrane protein PhoE of *Escherichia coli*. Eur. J. Biochem. 267, 3792–3800.

Johnson, A.E., Jensen, R.E., 2004. Barreling through the membrane. Nat. Struct. Mol. Biol. 11, 113–114.

Killian, J.A., 1998. Hydrophobic mismatch between proteins and lipids in membranes. Biochim. Biophys. Acta 1376, 401–415.

Kleinschmidt, J.H., den Blaauwen, T., Driessen, A., Tamm, L.K., 1999a. Outer membrane protein A of *E. coli* inserts and folds into lipid bilayers by a concerted mechanism. Biochemistry 38, 5006–5016.

Kleinschmidt, J.H., Tamm, L.K., 1996. Folding intermediates of a β-barrel membrane protein. Kinetic evidence for a multi-step membrane insertion mechanism. Biochemistry 35, 12993–13000.

Kleinschmidt, J.H., Tamm, L.K., 1999. Time-resolved distance determination by tryptophan fluorescence quenching: probing intermediates in membrane protein folding. Biochemistry 38, 4996–5005.

Kleinschmidt, J.H., Tamm, L.K., 2002. Secondary and tertiary structure formation of the β-barrel membrane protein OmpA is synchronized and depends on membrane thickness. J. Mol. Biol. 324, 319–330.

Kleinschmidt, J.H., Wiener, M.C., Tamm, L.K., 1999b. Outer membrane protein A of *E. coli* folds into detergent micelles, but not in the presence of monomeric detergent. Protein Sci. 8, 2065–2071.

Koronakis, V., Sharff, A., Koronakis, E., Luisi, B., Hughes, C., 2000. Crystal structure of the bacterial membrane protein TolC central to multidrug efflux and protein export. Nature 405, 914–919.

Kreusch, A., Schulz, G.E., 1994. Refined structure of the porin from *Rhodopseudomonas blastica*. Comparison with the porin from *Rhodobacter capsulatus*. J. Mol. Biol. 243, 891–905.

Kurisu, G., Zakharov, S.D., Zhalnina, M.V., Bano, S., Eroukova, V.Y., Rokitskaya, T.I., Antonenko, Y.N., Wiener, M.C., Cramer, W.A., 2003. The structure of BtuB with bound colicin E3 R-domain implies a translocon. Nat. Struct. Biol. 10, 948–954.

Kwok, R., Evans, E., 1981. Thermoelasticity of large lecithin bilayer vesicles. Biophys. J. 35, 637–652.

Ladokhin, A.S., 1999a. Analysis of protein and peptide penetration into membranes by depth-dependent fluorescence quenching: theoretical considerations. Biophys. J. 76, 946–955.

Ladokhin, A.S., 1999b. Evaluation of lipid exposure of tryptophan residues in membrane peptides and proteins. Anal. Biochem. 276, 65–71.

Ladokhin, A.S., Holloway, P.W., 1995. Fluorescence of membrane-bound tryptophan octyl ester: a model for studying intrinsic fluorescence of protein–membrane interactions. Biophys. J. 69, 506–517.

Laemmli, U.K., 1970. Cleavage of structural proteins during the assembly of the head of bacteriophage T4. Nature 227, 680–685.

Lazar, S.W., Kolter, R., 1996. SurA assists the folding of *Escherichia coli* outer membrane proteins. J. Bacteriol. 178, 1770–1773.

Lee, A.G., 2003. Lipid–protein interactions in biological membranes: a structural perspective. Biochim. Biophys. Acta 1612, 1–40.

Lewis, B.A., Engelman, D.M., 1983. Lipid bilayer thickness varies linearly with acyl chain length in fluid phosphatidylcholine vesicles. J. Mol. Biol. 166, 211–217.

Lis, L.J., McAlister, M., Fuller, N., Rand, R.P., Parsegian, V.A., 1982. Measurement of the lateral compressibility of several phospholipid bilayers. Biophys. J. 37, 667–672.

Locher, K.P., Rees, B., Koebnik, R., Mitschler, A., Moulinier, L., Rosenbusch, J.P., Moras, D., 1998. Transmembrane signaling across the ligand-gated FhuA receptor: crystal structures of free and ferrichrome-bound states reveal allosteric changes. Cell 95, 771–778.

Maier, C., Bremer, E., Schmid, A., Benz, R., 1988. Pore-forming activity of the Tsx protein from the outer membrane of *Escherichia coli* Demonstration of a nucleoside-specific binding site. J. Biol. Chem. 263, 2493–2499.

Markello, T., Zlotnick, A., Everett, J., Tennyson, J., Holloway, P.W., 1985. Determination of the topography of cytochrome b5 in lipid vesicles by fluorescence quenching. Biochemistry 24, 2895–2901.

Marsh, D., 1990. Lipid–protein interactions in membranes. FEBS Lett. 268, 371–375.

Marsh, D., Páli, T., 2001. Infrared dichroism from the X-ray structure of bacteriorhodopsin. Biophys. J. 80, 305–312.

McIntosh, T.J., Holloway, P.W., 1987. Determination of the depth of bromine atoms in bilayers formed from bromolipid probes. Biochemistry 26, 1783–1788.

Meyer, J.E., Hofnung, M., Schulz, G.E., 1997. Structure of maltoporin from *Salmonella typhimurium* ligated with a nitrophenylmaltotrioside. J. Mol. Biol. 266, 761–775.

Oomen, C.J., Van Ulsen, P., Van Gelder, P., Feijen, M., Tommassen, J., Gros, P., 2004. Structure of the translocator domain of a bacterial autotransporter. EMBO J. 23, 1257–1266.

Parsegian, V.A., Fuller, N., Rand, R.P., 1979. Measured work of deformation and repulsion of lecithin bilayers. Proc. Natl. Acad. Sci. U.S.A. 76, 2750–2754.

Pautsch, A., Schulz, G.E., 1998. Structure of the outer membrane protein A transmembrane domain. Nat. Struct. Biol. 5, 1013–1017.

Pautsch, A., Schulz, G.E., 2000. High-resolution structure of the OmpA membrane domain. J. Mol. Biol. 298, 273–282.

Pautsch, A., Vogt, J., Model, K., Siebold, C., Schulz, G.E., 1999. Strategy for membrane protein crystallization exemplified with OmpA and OmpX. Proteins 34, 167–172.

Piknova, B., Marsh, D., Thompson, T.E., 1997. Fluorescence quenching and electron spin resonance study of percolation in a two-phase lipid bilayer containing bacteriorhodopsin. Biophys. J. 72, 2660–2668.

Pocanschi, C.L., Apell, H.-J., Puntervoll, P., Høgh, B.T., Jensen, H.B., Welte, W., Kleinschmidt, J., 2006. The major outer membrane protein of *Fusobacterium nucleatum* (FomA) folds and inserts into lipid bilayers via parallel folding pathways. J. Mol. Biol. 355, 548–561.

Prieto, M.J., Castanho, M., Coutinho, A., Ortiz, A., Aranda, F.J., Gomez-Fernandez, J.C., 1994. Fluorescence study of a derivatized diacylglycerol incorporated in model membranes. Chem. Phys. Lipids 69, 75–85.

Prince, S.M., Achtman, M., Derrick, J.P., 2002. Crystal structure of the OpcA integral membrane adhesin from *Neisseria meningitidis*. Proc. Natl. Acad. Sci. U.S.A. 99, 3417–3421.

Puntervoll, P., Ruud, M., Bruseth, L.J., Kleivdal, H., Høgh, B.T., Benz, R., Jensen, H.B., 2002. Structural characterization of the fusobacterial non-specific porin FomA suggests a 14-stranded topology, unlike the classical porins. Microbiology 148, 3395–3403.

Rawicz, W., Olbrich, K.C., McIntosh, T., Needham, D., Evans, E., 2000. Effect of chain length and unsaturation on elasticity of lipid bilayers. Biophys. J. 79, 328–339.

Rodionova, N.A., Tatulian, S.A., Surrey, T., Jähnig, F., Tamm, L.K., 1995. Characterization of two membrane-bound forms of OmpA. Biochemistry 34, 1921–1929.

Rouviere, P.E., Gross, C.A., 1996. SurA, a periplasmic protein with peptidyl-prolyl isomerase activity, participates in the assembly of outer membrane porins. Genes Dev. 10, 3170–3182.

Schirmer, T., Keller, T.A., Wang, Y.F., Rosenbusch, J.P., 1995. Structural basis for sugar translocation through maltoporin channels at 3, 1 A resolution. Science 267, 512–514.

Schulz, G.E., 2002. The structure of bacterial outer membrane proteins. Biochim. Biophys. Acta 1565, 308–317.

Schwede, T., Kopp, J., Guex, N., Peitsch, M.C., 2003. SWISS-MODEL: an automated protein homology-modeling server. Nucl. Acids Res. 31, 3381–3385.

Schweizer, M., Hindennach, I., Garten, W., Henning, U., 1978. Major proteins of the *Escherichia coli* outer cell envelope membrane. Interaction of protein II with lipopolysaccharide. Eur. J. Biochem. 82, 211–217.

Snijder, H.J., Ubarretxena-Belandia, I., Blaauw, M., Kalk, K.H., Verheij, H.M., Egmond, M.R., Dekker, N., Dijkstra, B.W., 1999. Structural evidence for dimerization-regulated activation of an integral membrane phospholipase. Nature 401, 717–721.

Song, L., Hobaugh, M.R., Shustak, C., Cheley, S., Bayley, H., Gouaux, J.E., 1996. Structure of staphylococcal alpha-hemolysin, a heptameric transmembrane pore. Science 274, 1859–1866.

Surrey, T., Jähnig, F., 1992. Refolding and oriented insertion of a membrane protein into a lipid bilayer. Proc. Natl. Acad. Sci. U.S.A. 89, 7457–7461.

Surrey, T., Jähnig, F., 1995. Kinetics of folding and membrane insertion of a β-barrel membrane protein. J. Biol. Chem. 270, 28199–28203.

Surrey, T., Schmid, A., Jähnig, F., 1996. Folding and membrane insertion of the trimeric β-barrel protein OmpF. Biochemistry 35, 2283–2288.

van den Berg, B., Black, P.N., Clemons Jr., W.M., Rapoport, T.A., 2004. Crystal structure of the long-chain fatty acid transporter FadL. Science 304, 1506–1509.

Vandeputte-Rutten, L., Bos, M.P., Tommassen, J., Gros, P., 2003. Crystal structure of Neisserial surface protein A (NspA), a conserved outer membrane protein with vaccine potential. J. Biol. Chem. 278, 24825–24830.

Vandeputte-Rutten, L., Kramer, R.A., Kroon, J., Dekker, N., Egmond, M.R., Gros, P., 2001. Crystal structure of the outer membrane protease OmpT from *Escherichia coli* suggests a novel catalytic site. EMBO J. 20, 5033–5039.

Vogel, H., Jähnig, F., 1986. Models for the structure of outer-membrane proteins of *Escherichia coli* derived from Raman spectroscopy and prediction methods. J. Mol. Biol. 190, 191–199.

Vogt, J., Schulz, G.E., 1999. The structure of the outer membrane protein OmpX from *Escherichia coli* reveals possible mechanisms of virulence. Struct. Fold. Des. 7, 1301–1309.

Voulhoux, R., Bos, M.P., Geurtsen, J., Mols, M., Tommassen, J., 2003. Role of a highly conserved bacterial protein in outer membrane protein assembly. Science 299, 262–265.

Wang, Y.F., Dutzler, R., Rizkallah, P.J., Rosenbusch, J.P., Schirmer, T., 1997. Channel specificity: structural basis for sugar discrimination and differential flux rates in maltoporin. J. Mol. Biol. 272, 56–63.

Weiss, M.S., Kreusch, A., Schiltz, E., Nestel, U., Welte, W., Weckesser, J., Schulz, G.E., 1991. The structure of porin from *Rhodobacter capsulatus* at 1.8 Å resolution. FEBS Lett. 280, 379–382.

Weiss, M.S., Schulz, G.E., 1992. Structure of porin refined at 1.8 Å resolution. J. Mol. Biol. 227, 493–509.

Werner, J., Misra, R., 2005. YaeT (Omp85) affects the assembly of lipid-dependent and lipid-independent outer membrane proteins of *Escherichia coli*. Mol. Microbiol. 57, 1450–1459.

Wiener, M.C., White, S.H., 1991. Transbilayer distribution of bromine in fluid bilayers containing a specifically brominated analogue of dioleoylphosphatidylcholine. Biochemistry 30, 6997–7008.

Williamson, I.M., Alvis, S.J., East, J.M., Lee, A.G., 2002. Interactions of phospholipids with the potassium channel KcsA. Biophys. J. 83, 2026–2038.

Ye, J., van den Berg, B., 2004. Crystal structure of the bacterial nucleoside transporter Tsx. EMBO J. 23, 3187–3195.

Yue, W.W., Grizot, S., Buchanan, S.K., 2003. Structural evidence for iron-free citrate and ferric citrate binding to the TonB-dependent outer membrane transporter FecA. J. Mol. Biol. 332, 353–368.

Zeth, K., Diederichs, K., Welte, W., Engelhardt, H., 2000. Crystal structure of Omp32, the anion-selective porin from *Comamonas acidovorans*, in complex with a periplasmic peptide at 2.1 Å resolution. Struct. Fold. Des. 8, 981–992.